Cylindrical Micelles from the Aqueous Self-Assembly of an Amphiphilic Poly(ethylene oxide)–*b*-Poly(ferrocenylsilane) (PEO-*b*-PFS) Block Copolymer with a Metallo-Supramolecular Linker at the Block Junction

Jean-François Gohy,[a] Bas G. G. Lohmeijer,[b] Alexander Alexeev,[b] Xiao-Song Wang,[c] Ian Manners,*[c] Mitchell A. Winnik,*[c] and Ulrich S. Schubert*[b]

Abstract: A supramolecular AB diblock copolymer has been prepared by the sequential self-assembly of terpyridine end-functionalized polymer blocks by using Ru^{III}/Ru^{II} chemistry. By this synthetic strategy a hydrophobic poly(ferrocenylsilane) (PFS) was attached to a hydrophilic poly(ethylene oxide) (PEO) block to give an amphiphilic metallo-supramolecular diblock copolymer (PEO/PFS block ratio 6:1). This compound was used to form micelles in water that were characterized by a combination of dynamic and static light scattering, transmission electron microscopy, and atomic force microscopy. These complementary techniques showed that the copolymers investigated form rod-like micelles in water; the micelles have a constant diameter but are rather polydisperse in length, and light scattering measurements indicate that they are flexible. Crystallization of the PFS in these micelles was observed by differential scanning calorimetry, and is thought to be the key behind the formation of rod-like structures. The cylindrical micelles can be cleaved into smaller rods whenever the temperature of the solution is increased or they are exposed to ultrasound.

Keywords: block copolymers · micelles · poly(ferrocenylsilane)s · self-assembly · supramolecular chemistry

Introduction

Amphiphilic block copolymers comprise hydrophobic, water-insoluble blocks that aggregate into micellar cores and hydrophilic, water-soluble blocks that extend into the water phase and prevent the aggregates from being precipitated.[1] The characteristic dimensions of such aggregates, called “block copolymer micelles”, are in the nanometer range.[2] Such nanosized domains dispersed in water have been the focus of much interest, mainly because they can serve as nanoreactors, for example, for the production of colloidally stable (semi)-conducting nanoparticles[3] or as reservoirs for the transport of biologically active molecules such as DNA, enzymes, or drugs.[4–7]

The morphology and size of block copolymer micelles is basically related to the chemical composition of the copolymer and to the relative volume ratio of the two blocks.[8] Two extreme situations can be considered: block copolymers containing a minor hydrophobic block generally form spherical star-like micelles,[9] whereas copolymers with major hydrophobic blocks form the so-called crew-cut micelles[10] with various morphologies including rods, tubules, and vesicles, and with more complex, intricate morphologies.[11] Star-like micelles can generally be prepared by direct dissolution of the bulk copolymer in water, leading to structures close to the thermodynamic equilibrium, while use of an organic nonselective co-solvent first is needed for the preparation of crew-cut micelles.[12] Aggregation is then caused by the addition of a critical amount of water, and the final micelles are

---

[a] Prof. Dr. J.-F. Gohy
Unité de Chimie des Matériaux Inorganiques et Organiques (CMAT)
and Research Center in Micro- and
Nano-Materials and Electronic Devices (CERMIN)
Université Catholique de Louvain, Place L. Pasteur 1
1348 Louvain-la-Neuve (Belgium)

[b] Ir. B. G. G. Lohmeijer, Dr. A. Alexeev, Prof. Dr. U. S. Schubert
Laboratory of Macromolecular Chemistry and Nanoscience
Center for Nanomaterials
Eindhoven University of Technology and Dutch Polymer Institute
P.O. Box 513, 5600 MB Eindhoven (The Netherlands)
Fax: (+31) 40-2474186
E-mail: u.s.schubert@tue.nl

[c] Dr. X.-S. Wang, Prof. Dr. I. Manners, Prof. Dr. M. A. Winnik
Department of Chemistry, University of Toronto
80 St. George St., Toronto, Ontario M5S 3H6 (Canada)
Fax: (+1) 416 978-8775 or
Fax: (+1) 416 978-0541
E-mail: imanners@chem.utoronto.ca
mwinnik@chem.utoronto.ca

DOI: 10.1002/chem.200400222

collected in pure water by gradual elimination of the organic co-solvent by dialysis. This procedure leads to kinetically frozen block copolymer micelles, far from the thermodynamic equilibrium. Nevertheless, aqueous block copolymer micelles with nonspherical morphologies have also been obtained by direct dissolution of the bulk copolymer in water.[13]

Among the possible morphologies, rod-like or cylindrical micelles are of special interest because they can lead to conducting nanowires after metallization. (Semi)-conducting nanowires have also been obtained from the metallization of branched copolymers, as illustrated by the work of Schmidt et al.[14] as well as Müller and co-workers.[15] Simple polyelectrolyte chains adsorbed on a surface in a stretched conformation have also proven to be good candidates for the formation of metallic nanowires.[16] It is thus possible to use these polymeric precursors for the fabrication of metallic nanowires of different characteristic sizes.

Various approaches have been used to prepare micelles with cylindrical morphology. Selected examples can be found in the work of Antonietti et al.,[17] Liu and co-workers,[18] Möller et al.,[19] Bates and co-workers,[13,20] and others. Block copolymers containing PFS blocks have been used successfully to prepare, in organic solvents, cylindrical micelles whose core was formed by the self-assembly of the PFS blocks.[21] Such copolymers are of special interest in nanotechnology because they possess interacting metal ions in the polymer chains that can lead to charge-transport materials, or they can act as precursors to ceramics, including superparamagnetic nanoclusters formed by pyrolysis.[22]

Recently, we have introduced a novel type of amphiphilic block copolymer, namely metallo-supramolecular block copolymers.[23] In these compounds, the hydrophilic and hydrophobic blocks are not linked together by a covalent bond, but by a supramolecular bis(2,2′:6′,2″-terpyridine)ruthenium(II) complex. The associating behavior of amphiphilic metallo-supramolecular block copolymers in water has also been described very recently,[24] when it was demonstrated that the bis(2,2′:6′,2″-terpyridine)ruthenium(II) complex was very stable in aqueous solutions even at extreme pH values, when salt was added, or when the temperature of the solution was increased.[25] No ligand exchange was observed and the structural integrity of the metallo-supramolecular amphiphilic copolymers was maintained on a timescale of over one year. Nevertheless, it was still possible to open the complex under certain experimental conditions and this special property was used specifically to release the coronal chains of metallo-supramolecular micelles.[26] As a consequence, new opportunities for the application of such metallo-supramolecular block copolymers in nanotechnology can be opened up.[27]

Here we report the synthesis of a new type of amphiphilic diblock copolymer that consists of a PEO hydrophilic block linked to a hydrophobic PFS block through a bis(2,2′:6′,2″-terpyridine)ruthenium(II) complex, and we describe in detail formation of cylindrical aqueous micelles from this copolymer (Scheme 1).

Results and Discussion

The formation of micelles has been reported previously for block copolymers containing PFS segments. These PFS blocks were combined with polystyrene (PS), poly(dimethylsiloxane) (PDMS), or polyisoprene (PI).[21,28–30] As a result, diblock and ABA triblock copolymer architectures were prepared. Micelles were formed in organic solvents such as *n*-hexane, in which the PFS blocks are insoluble and self-aggregate into a micellar core while a micellar corona is formed by the PI or PDMS block. Amphiphilic diblock copolymers have also been prepared recently in which the PFS blocks form the micellar core, while chains of the water-soluble neutral polymers PEO[31] or poly(*N*,*N*-dimethylaminoethyl methacrylate) (PDMAEMA)[32] extend into the water phase. Various morphologies were observed for these micelles: spheres, rods, or semi-hollow nanotubes. In the case of PFS block polymers in alkane solvents, spheres were observed when the PFS block was amorphous whereas cylindrical morphologies were formed for crystallizable PFS blocks. A major clue that the crystallinity of the PFS block is the driving force for the formation of cylindrical micelles in PFS block copolymers was provided by experiments in which spherical micelles were formed in decane above the normal melting temperature of the crystallizable PFS block. Under these circumstances, spherical star-like micelles were observed. In this contribution, we describe the first example of the formation in water of cylindrical micelles from PFS-containing amphiphilic block copolymers based on PEO. This polymer is unique in that the two blocks are coupled through a metallo-supramolecular junction.

Synthesis of PFS_{12}-[Ru]-PEO_{70} copolymer: The ring-opening polymerization (ROP) of strained monomeric silicon-bridged [1]ferrocenophanes is a well established route to poly(ferrocenylsilane)s. This polymerization has been carried out under living conditions by anionic ROP. Monochelic hydroxy-functional PFS was obtained by using a protected initiator, (*tert*-butyldimethylsilyloxy)-1-propyllithium (*tert*-BDMSPrLi), whereby after polymerization the *tert*-BDMS group was hydrolyzed in the presence of $[NBu_4]F$ at room temperature. This reaction sequence led to **3**,[32,33] which subsequently reacted with an isocyanate-functionalized terpyridine, **2**. Other experimental conditions reported earlier for the terpyridine functionalization of hydroxy-terminated polymers either oxidized part of the backbone or did not lead to full conversion of the hydroxy to the terpyridine end-group.[23] Therefore, the amino group of an amino-functionalized terpyridine (**1**) was converted into an isocyanate group by reaction with di(*tert*-butyl tricarbonate).[34] In the presence of a catalytic amount of dibutyltin dilaurate (DBTDL), the hydroxy group of the PFS backbone was fully converted to a urethane bond, as judged from ^{1}H NMR as well as from IR spectroscopy. Purification by preparative size exclusion chromatography (SEC) led to the terpyridine-functionalized PFS **4**.

A terpyridine ω-functionalized PEO was prepared and reacted with $RuCl_3$ to selectively form a mono(terpyridine)ruthenium(III) complex **5**.[23] The SEC curve of **5**, measured

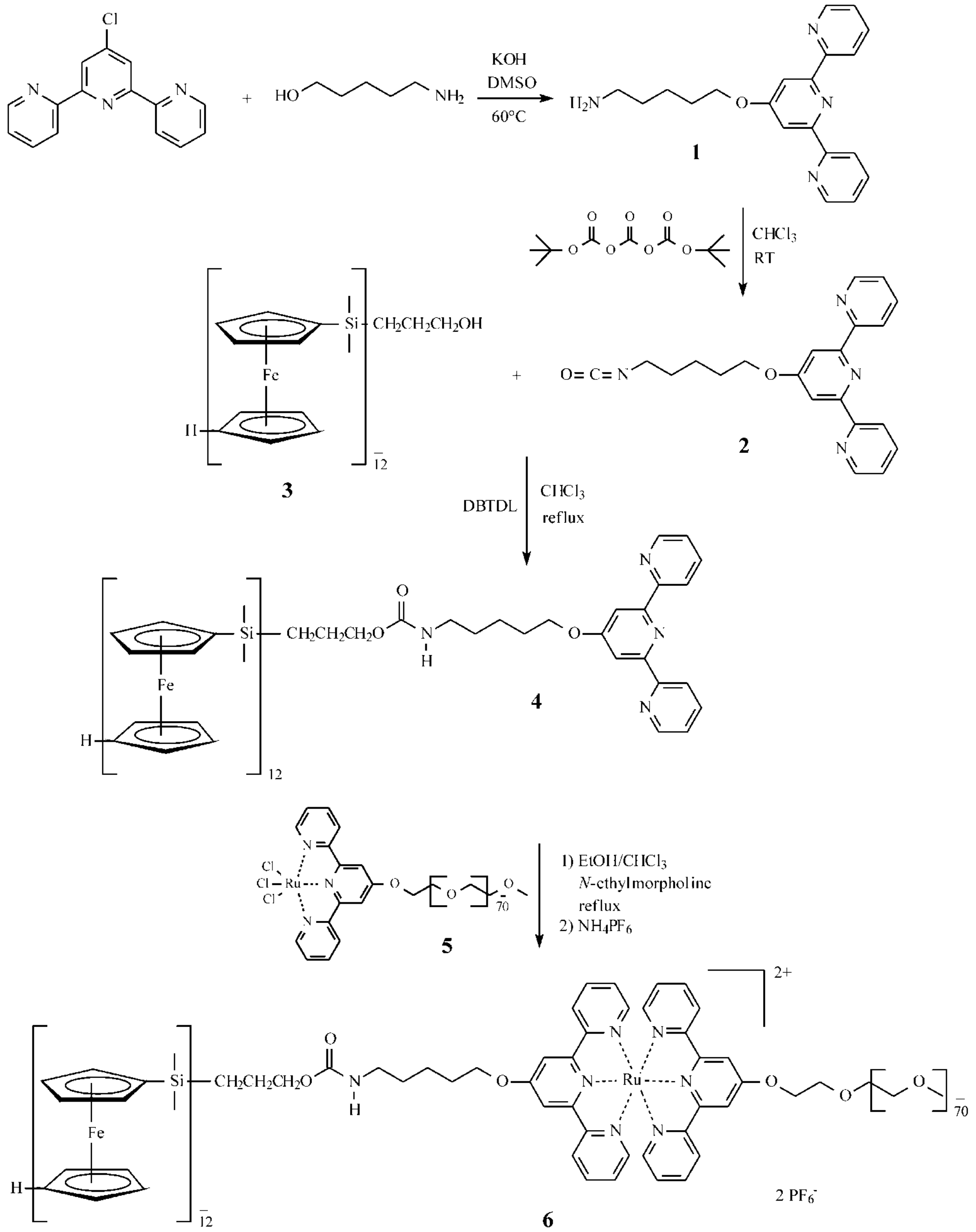

Scheme 1. Synthesis of the metallo-supramolecular amphiphilic PFS_{12}-[Ru]-PEO_{70} block copolymer **6**.

with a diode array detector, is shown in Figure 1. This technique allowed us to measure the entire UV/Vis spectrum at each elution time. The metal-to-ligand charge transfer (MLCT) band observed at 390 nm provides clear evidence for the exclusive formation of the mono(terpyridine)ruthenium(III) complex, for which the terpyridine signals in the ^{1}H NMR spectrum are no longer observed as the metal complex is paramagnetic.

In the final step, the PFS block **4** reacted with the PEO block **5** under reducing conditions, to form the bis(terpyridine)ruthenium(II) complex **6** selectively through a self-assembly process. The SEC curve of **6** is also shown in Figure 1. Compared with the precursor **5**, the curve of **6** is now shifted to lower elution volume due to the increase in molecular weight. No extra peaks at higher elution volumes have been observed, indicating the absence of both uncomplexed polymer blocks and fragmented PFS in **6**. Moreover, the maximum of the MLCT band is now observed at 490 nm, indicating the successful formation of the bis(terpyridine)ruthenium(II) complex.[35a] The terpyridine signals in the ^{1}H NMR spectrum are shifted when compared to the uncomplexed terpyridine-functionalized polymer blocks. The MALDI-TOF mass spectrum (Figure 2) reveals, apart from **6**, the presence of the different blocks of the supramolecular block copolymer, indicating that the supramolecular connection is partly broken during the MALDI process; this was observed for other metallo-supramolecular block copolymers as well.[35b] In conclusion, these experimental results show the exclusive formation of compound **6**.

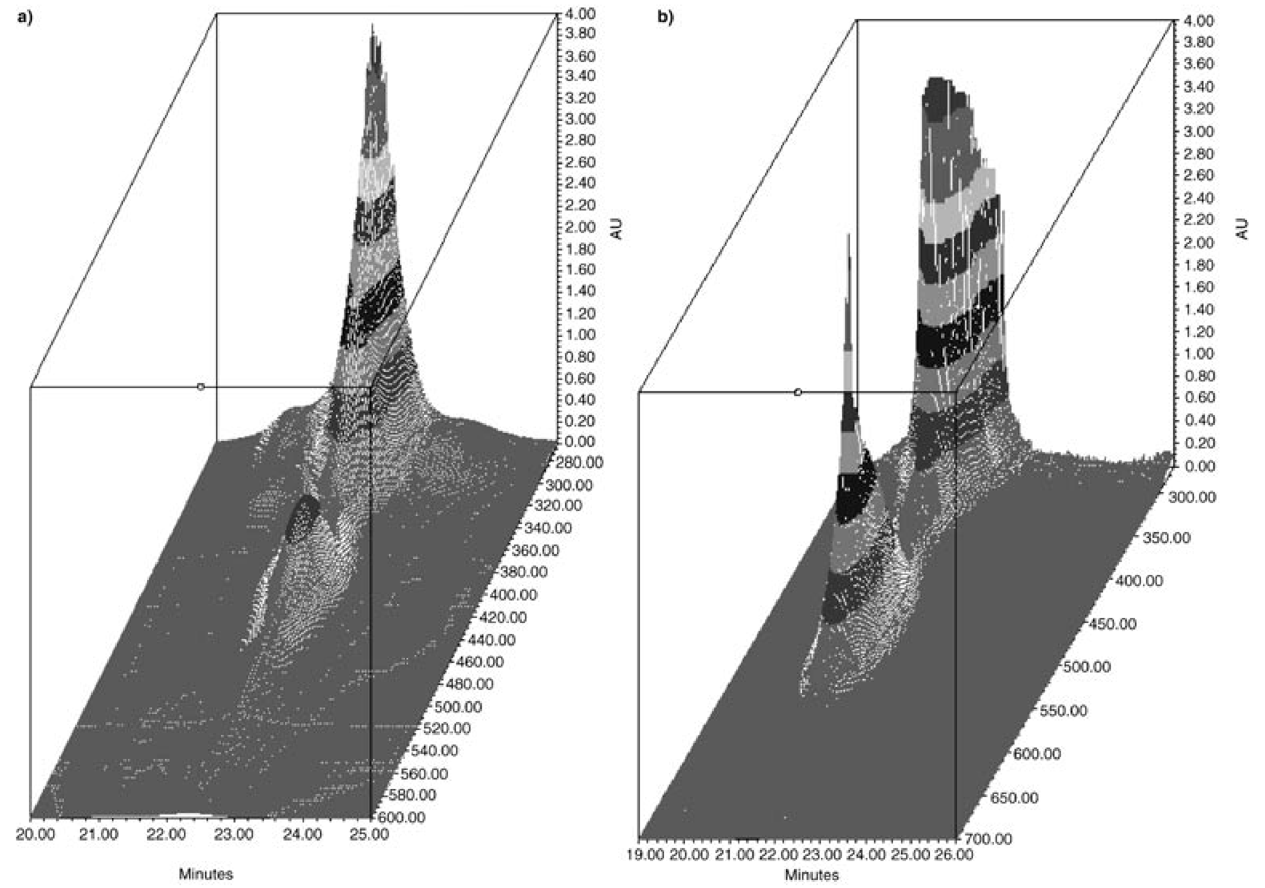

Figure 1. SEC curves, measured with a diode array detector, for a) PEO_{70}-[$RuCl_3$] (**5**); b) PFS_{12}-[Ru]-PEO_{70} (**6**).

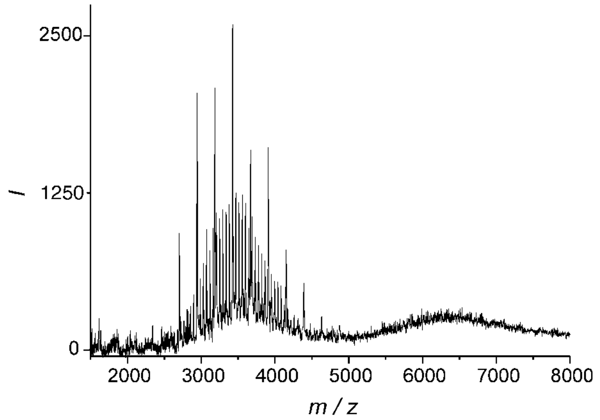

Figure 2. MALDI-TOF mass spectrum of PFS_{12}-[Ru]-PEO_{70} **6**: The three distributions arise from breakage of the supramolecular linkage in the MALDI process, but illustrate nicely the presence of the PEO block ($\Delta m/z$ 44), the PFS block ($\Delta m/z$ 242), and the metallo-supramolecular diblock (broad peak at m/z 6300).

Micellization of PFS_{12}-[Ru]-PEO_{70}: The bulk sample **6** was poorly soluble in water. The method previously introduced by Eisenberg et al. was therefore used for the preparation of the micelles.[10–12] Compound **6** was initially dissolved in *N,N*-dimethylformamide, a common solvent for both blocks. Water was then added gradually. The scattered light intensity was monitored as a function of the amount of water added. A sharp increase in scattered intensity was noted when the critical water concentration (cwc) was reached.[36] At the same time, foam was observed when the solution was being shaken, indicating that the DMF/H_2O mixture was no longer a good solvent for both blocks and that the water-insoluble blocks (PFS) were starting to aggregate into micellar cores and the block copolymer was then behaving as a macro-surfactant. The cwc (0.55 mL for 1 mL of a 50 $g\,L^{-1}$ copolymer DMF solution) was substantially higher than the values observed for crew-cut micelles, in agreement with a larger volume ratio for the hydrophilic block of **6**. Additional water was added beyond the cwc, in order to freeze-in the morphology, as previously discussed by Eisenberg et al.[10–12] Finally DMF was eliminated by dialysis against water.

Light scattering of PFS_{12}-[Ru]-PEO_{70} aqueous micelles: The aqueous micelles formed by **6** were first analyzed by static light scattering (SLS). Since these micelles can be regarded as kinetically frozen aggregates rather than equilibrium micelles, the concentration of free copolymer chains should be extremely low for the solutions investigated. Their contribution to the scattering signals was therefore neglected. The angular dependence of the SLS data (extrapolated to zero concentration) was investigated (Figure 3). The apparent M_w of the micelles was determined from the intercept of the straight line shown in Figure 3 with the *y* axis. Its value, $(1.52 \pm 0.06) \times 10^7\,g\,mol^{-1}$, leads to a mean aggregation

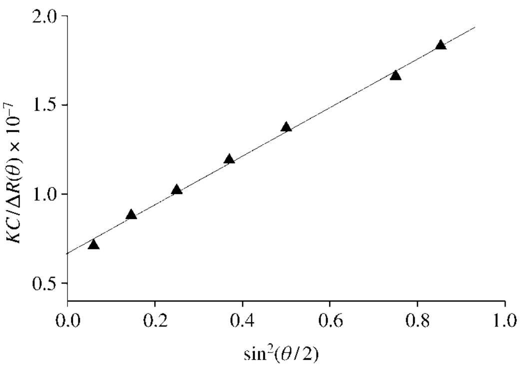

Figure 3. Angular dependence of the SLS data extrapolated to zero concentration for PFS_{12}-[Ru]-PEO_{70} aqueous micelles.

number of about 2500 chains per micelle and is too high for spherical micelles, which have aggregation numbers that are typically around 100.[2] The radius of gyration of the micelles, $R_g = (55 \pm 4)$ nm, was determined from the slope of the angular dependence of the SLS signal; it also is not in agreement with the presence of spherical block copolymer micelles.

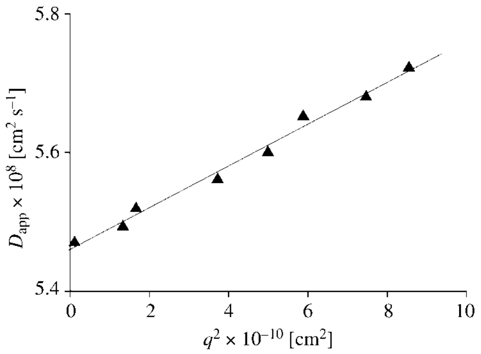

Figure 4. Angular dependence of the apparent diffusion coefficient for PFS_{12}-[Ru]-PEO_{70} aqueous micelles ($C = 1\,gL^{-1}$).

Dynamic light scattering (DLS) was used to determine the mean hydrodynamic diameter D_h of the aqueous micelles formed by **6**. The diffusion coefficient for these micelles was found to be approximately $5.5 \times 10^{-8}\,cm^2 s^{-1}$, corresponding to a mean D_h of (89 ± 1) nm (Stokes–Einstein approximation), while the polydispersity was calculated from the Γ_1/Γ_2^2 ratio to be (0.21 ± 0.02).[37] The angular dependence of the apparent diffusion coefficient was also measured. The slope of the angular dependence of D_{app} is related to the shape of the diffusing species and was found to be 0.029, consistent with the value predicted for rod-like structures (0.03) (Figure 4).[38] However, the CONTIN size distribution histogram related to the micelles formed by **6** systematically shows a unimodal distribution (Figure 5). Rod-like micelles are usually characterized by two or more relaxation modes, as a result of the coupling of translational and rotational diffusion.[39] An unimodal distribution can however be observed for very flexible rods.[21a]

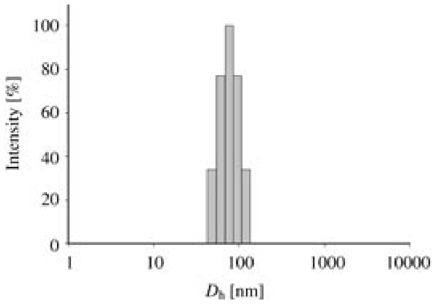

Figure 5. CONTIN size distribution histogram for PFS_{12}-[Ru]-PEO_{70} micelles in water ($C = 1\,gL^{-1}$).

Information about the inner density profile of the micellar structure can be obtained by considering the R_g/R_h ratio.[38] Its theoretical value for monodisperse hard spheres is 0.775, whereas it is 1.5 for Gaussian chains. In the case of cylindrical structures, the R_g/R_h ratio depends strongly on the length and thickness of the micelles.[21a] It was found to be 1.24 for the micelles formed by **6**, which is similar to the R_g/R_h value of 1.25 previously reported by Liu et al. for cylindrical micelles formed by PS-*b*-poly(2-cinnamoylethyl methacrylate) with a cross-linked core in toluene.[18a] Very similar conclusions were drawn from the study of PFS-*b*-PDMS micelles in *n*-hexane.[21a] In summary, light scattering investigations on the aqueous micelles formed by PFS_{12}-[Ru]-PEO_{70} strongly support the formation of flexible cylindrical or rod-like structures.

Morphological investigation of PFS_{12}-[Ru]-PEO_{70} aqueous micelles: Transmission electron microscopy (TEM) has been used as a tool to characterize the micelles formed from sample **6**. Since the TEM images were obtained for micelles dried on a Formvar film, the morphology of the micelles may have been modified during the drying process, but this effect was thought to be limited for the micelles under investigation because they are essentially frozen aggregates that contain crystallizable PFS blocks. Rod-like micelles were observed by TEM everywhere on the grids, as illustrated in Figure 6a for the sample without staining. The electronic contrast originates from the PFS core, which contains iron and is surrounded by the bis(terpyridine)ruthenium(II) complexes. The diameter of the core, (6 ± 1) nm, was found to be constant for all these rods. This is consistent with the dimension of a core formed by the very short PFS blocks. The length of the rods is highly variable; a mean value of (438 ± 12) nm has been calculated from image analysis. Compared with R_g and R_h values, the contour length of the cylindrical micelles as measured by TEM is much greater. This is in agreement with the formation of highly flexible cylindrical micelles in solution.

The micelles were also negatively contrasted with phosphotungstic acid (see Figure 6b). Since the sample was prepared in two steps (first, deposition of the micelle and drying; second, deposition of a drop of the contrasting agent), the contrasting agent was likely to be located outside the corona of the micelles. Provided that it did not penetrate too far into the PEO corona, the (core+corona) dimension

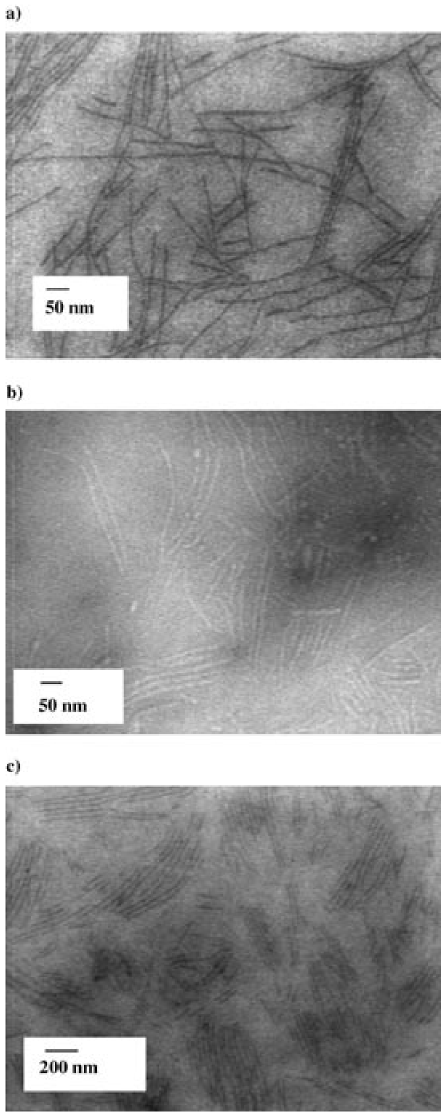

Figure 6. TEM images for PFS_{12}-[Ru]-PEO_{70} micelles observed a) without staining; b) with negative staining; c) bundles of parallel cylindrical micelles (no staining).

of the micelles could be determined: in the dried state the value measured was (11 ± 1.5) nm. The thickness of the dried, collapsed PEO corona was therefore 2.5 nm. The cylindrical micelles tend to form bundles, in which they are close packed and oriented parallel to each other (Figure 6c). These aggregates have not been detected in the micellar solutions by light scattering, and are therefore thought to be formed during the process of drying during TEM sample preparation. This nematic type of structure is a normal feature of species with a high aspect ratio at high concentrations. An average aggregation number of 3600 and a molecular weight of 2.25×10^7 Da have been calculated, as described elsewhere for other PFS-containing micelles,[28] from the average dimension of the cylindrical micelles. These values are substantially higher than those determined from SLS measurements, in agreement with the previously reported results.[28]

Atomic force microscopy (AFM) measurements of micelles cast from a dilute micellar solution on a silicon wafer revealed the presence of cylindrical micelles (data not shown), in agreement with the LS and TEM results. Image analysis of these AFM images showed that these micelles were polydisperse in length, with a height of (13 ± 2) nm and a lateral diameter of (21 ± 2) nm. The height of the micelles was in good agreement with TEM results ((core+corona) dimension of (11 ± 1.5) nm in the dried state). The lateral dimension measured by AFM was greater than that obtained from TEM images. This discrepancy could be explained by tip-convolution effects, which are commonly observed for AFM investigations on isolated micelles deposited on a substrate. Bundles formed by parallel cylindrical micelles have also been commonly observed in AFM images, in agreement with the TEM results.

Formation of cylindrical micelles for the PFS_{12}-[Ru]-PEO_{70} sample: For copolymers in which a flexible block is linked to a crystallizable core-forming block, the formation of cylindrical micelles is caused by the particular orientation of the core-forming chains resulting from the crystallization process. PFS is a core-forming block that is characterized by a strong propensity to crystallize.[22] This crystallization process has been demonstrated previously to be at the origin of the cylindrical micelles formed by PFS-containing block copolymers in alkane solvents.[21] In order to establish whether the aqueous micelles formed by sample **6** contained a crystallized PFS core, we first lyophilized the micelles in order to maintain the nanostructures in the bulk state initially formed in solution. Samples of these dried micelles were then examined by differential scanning calorimetry (DSC). Two endotherms were observed in the DSC curves. The first (52.8 ± 0.1 °C, $\Delta H = 57.4 \pm 0.4\,\mathrm{J\,g^{-1}}$) can be assigned to the melting of the PEO chains which crystallized during the lyophilization process, while the second (122.2 ± 0.2 °C, $\Delta H = 10 \pm 0.2\,\mathrm{J\,g^{-1}}$) corresponds to the melting of the PFS core. The presence of a crystallized PFS core in micelles formed by sample **6** is therefore confirmed. Aqueous micelles have been prepared previously from PFS-*b*-PEO diblock copolymers with a covalent bond between the two constituent blocks. The degrees of polymerization of both blocks in this PFS-*b*-PEO sample were essentially the same as those of the PFS_{12}-[Ru]-PEO_{70} under investigation. Micelles were prepared by direct dissolution of the PFS-*b*-PEO sample in water but large polydisperse spherical micelles were observed for this sample.[31] Clearly the D_h measured by DLS (~160 nm) and the diameter of the micelles measured by TEM (~50 nm) for these spherical micelles were too large to be consistent with dense spherical micelles at equilibrium. From the comparison of PFS-*b*-PEO and PFS_{12}-[Ru]-PEO_{70} micelles, it can be concluded that the presence of the bis(terpyridine)ruthenium(II) complex decreases the solubility of the copolymer in water and has a beneficial effect on the crystallization of the PFS blocks. However, aqueous cylindrical micelles whose characteristic features are quite similar to those of PFS-[Ru]-PEO micelles have recently been reported for a PFS-*b*-PDMAEMA copolymer.[32] The role of the bis(terpyridine)ruthenium(II) complexes in determining the ability of the PFS blocks to crystallize is therefore still unclear.

Stability of the PFS_{12}-[Ru]-PEO_{70} aqueous micelles: Metallo-supramolecular micelles with a polystyrene core have been reported to be extremely stable in water with respect to salt concentration, temperature, and pH.[25] Nevertheless, previous results have demonstrated a strong tendency for the micelles to aggregate into large clusters.[24,25] Both the addition of salt and an increase in temperature dramatically increased the clustering of spherical micelles formed by PS-[Ru]-PEO.[24,25] The effect of the addition of salt and the increase in temperature have been investigated for the micellar solution formed by **6**. The effect of sonication has also been evaluated.

Salt was added to the micellar solution (KCl, 1 molL^{-1}) and the sample was equilibrated for 6 h before measurements were taken. The mean D_h was found to be (86 ± 1.5) nm and the polydispersity of the micelles was (0.21 ± 0.01). The slight decrease in micellar size in the presence of KCl (Figure 7a) can be attributed to the desolvation of PEO coronal chains in the presence of salt (salting-out effect). Upon addition of higher amounts of salt, flocculation was observed as a result of the reduced steric stabilization of the poorly solvated PEO chains.

To investigate the effect of temperature, the temperature of the bath surrounding the DLS equipment was raised. After thermal equilibration, the DLS data were collected. The characteristic size of the micelles was hardly affected below 70 °C: for example, D_h = 80 ± 2 nm and polydispersity = 0.18 ± 0.01 at 65 °C (Figure 7b). At higher temperatures, flocculation was again observed, in agreement with the desolvation of the PEO chains.

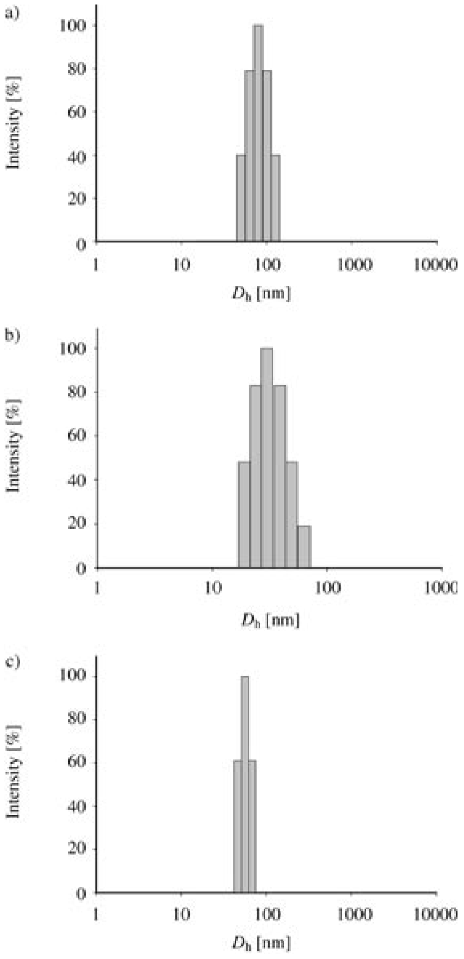

Figure 7. CONTIN size distribution histograms for PFS_{12}-[Ru]-PEO_{70} micelles (C = 0.5 gL^{-1}): a) in 1 molL^{-1} KCl; b) in water at 65 °C; c) in water after 2 h of ultrasonication.

After ultrasonication of the micellar solution for 2 h, a profound change in the micellar characteristic features was noted. The mean D_h dropped to 65 ± 1.2 nm while the polydispersity increased to 0.28 ± 0.02. The CONTIN size distribution histograms also indicated an important decrease in size (Figure 7c). A typical TEM image of the rods observed after ultrasonication is shown in Figure 8. The diameter of the PFS core (5 ± 1 nm) was not affected by this treatment but the rods were substantially shorter than those of the original sample. An average length of 138 ± 4 nm was calculated from a collection of TEM images of ultrasonicated rods: the aggregation number was reduced from 3600 to 1000. In a previous study on cylindrical micelles formed by PFS-*b*-PDMS copolymers in *n*-hexane, a similar ultrasonication resulted in a more significant decrease in the length of the cylindrical micelles. In contrast to our results, the polydispersity of the ultrasonicated rods was considerably lower than that of the initial PFS-*b*-PDMS cylindrical micelles. Electrostatic interactions occurring among bis(terpyridine)-ruthenium complexes and the associated counter-anions, studied recently by small-angle X-ray scattering on a metallo-supramolecular block copolymer melt,[39] could perhaps explain why metallo-supramolecular cylindrical micelles are more resistant to ultrasound-induced cleavage.

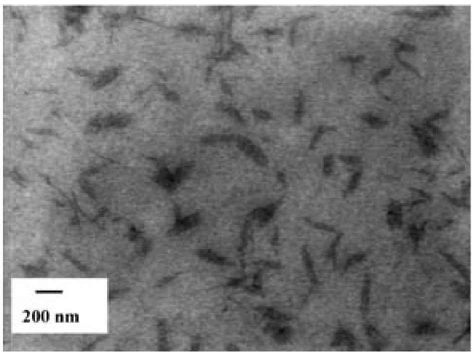

Figure 8. A typical TEM image for ultrasonicated PFS_{12}-[Ru]-PEO_{70} micelles observed without staining.

Summary

A metallo-supramolecular amphiphilic diblock copolymer has been prepared through the self-assembly of a terpyridine functionalized PEO with an organometallic PFS block bearing one terpyridine end-group. The exclusive formation of the diblock has been confirmed by a combination of various analytical techniques. Micelles were then prepared in water from this copolymer. Because the bulk sample could not be solubilized directly in water, the transient use of an organic nonselective solvent was required. Crystallization of the short PFS blocks occurred during the micellization process, resulting in the formation of cylindrical micelles. Static and dynamic light scattering results were both in agreement with the formation of highly flexible cylindrical micelles. These rod-like micelles were visualized by TEM and AFM and their characteristic dimensions were accordingly determined from a collection of images. The diameter of the PFS core and the thickness of the PEO corona were found to be very small, in agreement with the low degree of polymerization of the constituent polymer blocks, whereas the micelles were long (micrometer-sized cylindrical micelles were commonly observed in TEM or AFM images). An increase in temperature or in ionic strength resulted in decreased water solubility of the PEO block, which, in turn, caused flocculation of the micelles. Ultrasonic treatment resulted in shortening of the cylindrical micelles, while their diameter was not affected. Since the PFS cylindrical cores of these micelles are known to be useful for charge transport and are precursors to ferromagnetic nanostructures, these water-soluble substances are believed to be promising candidates for applications in nanotechnology.

Experimental Section

Equipment and materials: Chemicals were received from Aldrich, SyMO-Chem, and Shearwater and used without further purification. Synthesis of 4′-(1-aminopentyloxy)-2,2′;6′,2″-terpyridine[40] (**1**), α-hydrido-ω-hydroxy-polyferrocenylsilane,[32] (**3**) and PEO_{70}-$[RuCl_3]$[23] (**5**) are described elsewhere.

Solvents were bought from Biosolve. DMF and chloroform were dried over molecular sieves and DMSO was dried over BaO. For preparative SEC, Bio-Rad SX-1 beads swollen in CH_2Cl_2 and THF were used. ^1H NMR and ^{13}C NMR spectra, respectively, were recorded on a Varian Mercury spectrometer with frequencies of 400 and 100 MHz at 25 °C and on a Varian Gemini spectrometer with frequencies of 300 and 75 MHz at 25 °C. Chemical shifts are given downfield from TMS. UV/Vis spectra were recorded on a Perkin-Elmer Lambda 45P spectrophotometer. Matrix-assisted laser desorption/ionization mass spectra were obtained using dithranol as the matrix and NaI on a PerSeptive Biosystems Voyager DE PRO spectrometer using a layer-by-layer spotting technique. SEC on the ruthenium-containing polymers was performed on a Waters Styragel HT4 column 30 cm long and analyzed with an RI detector (Waters 1414) and a photo diode array detector (Waters 2915) with DMF as the eluent with NH_4PF_6 (5 $mol\,L^{-1}$) as additive to reduce column interactions at a flow of 0.5 $mL\,min^{-1}$ utilizing a Waters 1515 pump. Poly(methyl methacrylate) standards were used for calibration, since PS and PEO standards did not give good signal-to-noise ratios with DMF. SEC on the covalent polymers was conducted on a PL mixed D column 30 cm long and analyzed with an RI detector (Shimadzu RID-10A) and a UV/Vis detector (SPD-10Avp) at 275 nm with chloroform as the eluent with Et_3N (4 %) and isopropanol (2 %) as additives to reduce column interaction of the free terpyridine ligand at a flow of 1.0 $mL\,min^{-1}$ using a Shimadzu LC-10Avp pump. Polystyrene standards were used for calibration. IR spectra were measured on a Perkin-Elmer 1600 FT-IR in ATR mode. Dynamic and static light scattering was carried out on a Brookhaven Instruments Corp. BI-200 apparatus equipped with a BI-2030 digital correlator with 136 channels and a Spectra Physics He/Ne laser, wavelength $\lambda = 633$ nm. A refractive index matching bath of filtered decalin surrounded the scattering cell; the temperature was controlled at 25 °C. Toluene was used as a reference to determine the Rayleigh ratio. The refractive index increment ($dn/dC = 0.1134\ mL\,g^{-1}$ for the sample investigated) was measured with an Optilab DSP interferometric refractometer (Wyatt Technology) at 633 nm. All solutions were filtered with a 0.45 μm syringe filter before measurement. The reproducibility of the DLS results was checked by analyzing each sample at least ten times. The standard deviation between these independent measurements was less than 2 %.

TEM was carried out with a JEOL 2000 FX working at 200 kV and equipped with a CCD camera. The samples were prepared by drop-casting of a diluted (0.01 $g\,L^{-1}$) micellar solution on a Formvar-coated copper grid. No contrasting agent was used for the direct observation of the micelles. The micelles were further negatively contrasted with phosphotungstic acid ($H_3PO_4{\cdot}12\,WO_3$) by casting a drop of a diluted staining agent solution (0.1 $g\,L^{-1}$) on the previously prepared samples. Kontron KS 100 software was used to collect and analyze the TEM images. AFM measurements on a diluted micellar solution (0.01 $g\,L^{-1}$) cast on a silicon wafer were performed with a Digital Instruments Nanoscope IIIa Multimode operated in air in the tapping mode.

Differential scanning calorimetry was performed with a Perkin-Elmer Pyris 1 apparatus, calibrated with an indium standard at a heating rate of 10 $°C\,min^{-1}$. The micellar solution was freeze-dried, dried micelles (30 mg) were transferred to an aluminum pan, and then the DSC curve was recorded directly, starting from −50 °C.

Synthesis of 4′-(1-isocyanatopentyloxy)-2,2′;6′,2″-terpyridine (2): Di(*tert*-butyl) tricarbonate (0.823 g, 3.14 mmol) was stirred in dry chloroform (50 mL). After 15 min a solution of **1** (1.000 g, 2.99 mmol) in dry chloroform (50 mL) was added by syringe to the stirred solution. Stirring was continued for another 20 min, after which the solvent was evaporated in vacuo. No further purification of the remaining brown oil, which contained some excess tricarbonate, was attempted and the crude material was used as such. The oil was stored in the freezer (−25 °C) until further use (1.15 g, >99 %). ^1H NMR (300 MHz, $CDCl_3$, 25 °C): $\delta = 1.52$ (m, 2H; CH_2), 1.66 (m, 2H; CH_2), 1.86 (m, 2H; CH_2), 3.33 (t, $^3J(H,H) = 6.2$ Hz, 2H; CH_2NCO), 4.21 (t, $^3J(H,H) = 6.2$ Hz, 2H; OCH_2), 7.31 (ddd, $^3J(H,H) = 6.4$, $^4J(H,H) = 4.8$, $^5J(H,H) = 1.6$ Hz, 2H; $H_{5,5''}$), 7.84 (ddd, $^3J(H,H) = 7.6$, $^4J(H,H) = 6.2$, $^5J(H,H) = 1.6$ Hz, 2H; $H_{4,4''}$), 8.00 (s, 2H; $H_{3',5'}$), 8.60 (dt, $^3J(H,H) = 8.0$, $^4J(H,H) = 1.0$, $^5J(H,H) = 0.9$ Hz, 2H; $H_{3,3''}$), 8.67 (dt, $^3J(H,H) = 4.7$, $^4J(H,H) = 1.8$, $^5J(H,H) = 0.9$ Hz, 2H; $H_{6,6''}$); ^{13}C NMR (75 MHz, $CDCl_3$): $\delta = 23.0$ (C_γ), 28.3 (C_β), 30.8 (C_δ), 42.7 (C_α), 67.6 (C_ε), 107.2 ($C_{5,5''}$), 121.2 (N*C*O, $C_{4,4''}$), 123.7 ($C_{3,3''}$), 136.7 ($C_{3',5'}$), 148.9 ($C_{6,6''}$), 156.0 ($C_{2,2''}$), 157.0 ($C_{2',6'}$), 167.0 ppm ($C_{4'}$); IR (ATR): $\tilde{\nu} = 3055$, 2945, 2875 (CH tpy, alkyl CH_2); 2261 (NCO); 1600, 1582, 1563 cm^{-1} (C=C, C=N tpy).

Synthesis of α-hydrido-ω-terpyridinyl-polyferrocenylsilane (4): α-Hydrido-ω-hydroxy-polyferrocenylsilane (200 mg, 0.071 mmol), **3** (50 mg, 0.142 mmol), and a catalytic amount of DBTDL were stirred in dry chloroform (10 mL) at reflux. Stirring was continued overnight, after which the solvent was removed in vacuo. The crude product was purified by column chromatography (SiO_2, $CHCl_3$) and preparative SEC (Bio-Beads SX-1, CH_2Cl_2) and finally precipitated (105 mg, 46 %) from THF in hexanes. ^1H NMR (300 MHz, $CDCl_3$, 25 °C): $\delta = 0.70$–0.27 (m, 74H; $SiCH_2$, $SiCH_3$, PFS), 1.59 (m, 6H; CH_2), 1.88 (m, 2H; $tpyOCH_2CH_2$), 3.22 (m, 2H; CH_2NH), 4.32–3.89 (m, 99H; fc, PFS, $CH_2OC(=O)$), 4.37 (m, 2H; $tpyOCH_2$), 4.71 (s, 1H; NHCOO), 7.35 (dd, $^3J(H,H) = 8.0$, $^4J(H,H) = 5.2$ Hz, 2H; $H_{5,5''}$), 7.87 (td, $^3J(H,H) = 8.0z$, $^4J(H,H) = 1.8$ Hz, 2H; $H_{4,4''}$), 8.06 (s, 2H; $H_{3',5'}$), 8.67 (d, $^3J(H,H) = 8.0$ Hz, 2H; $H_{3,3''}$), 8.73 (d, $^3J(H,H) = 5.2$ Hz, 2H; $H_{6,6''}$); UV/Vis (CH_2Cl_2): λ_{max} (ε): 453 (1800), continuously increasing absorption from 369 to 245 nm (400–93 000 $mol^{-1}\,L\,cm^{-1}$); IR (ATR): $\tilde{\nu} = 3082$, 2954 (alkyl CH_2, CH tpy); 1721, 1515 (NHCOO); 1600, 1583, 1564 (C=C, C=N, tpy); 1249, 1163, 1034, 797, 767 cm^{-1} (PFS); GPC (RI): $M_n = 2700\ g\,mol^{-1}$, polydispersity index (PDI) = 1.13; MS (dithranol, MALDI-TOF): distribution with $\Delta(m/z) = 242$ Da, peak of highest intensity $m/z = 3080$; $M_n = 3150\ g\,mol^{-1}$, PDI = 1.03.

Synthesis of the PFS_{12}-[Ru]-PEO_{70} amphiphilic block copolymer (6): A solution of **4** (50 mg, 0.016 mmol) and **5** (52 mg, 0.015 mmol) was refluxed in a solvent mixture of chloroform and ethanol (4:1, 5 mL). After 30 min a catalytic amount of *N*-ethylmorpholine was added. Stirring was continued overnight, after which the solvent was evaporated in vacuo. The crude product was purified by preparative SEC (BioBeads SX-1, THF, followed by BioBeads SX-1, CH_2Cl_2) and precipitated from CH_2Cl_2 in hexanes (78 mg, 76 %). ^1H NMR (400 MHz, $CDCl_3$, 25 °C): $\delta = 0.70$–0.27 (m, 74H; $SiCH_2$, $SiCH_3$, PFS), 1.59 (m, 6H, CH_2), 1.72 (b, 2H; CH_2CH_2NHCOO), 2.00 (b, 2H; $tpyOCH_2CH_2CH_2$), 2.08 (b, 2H; $tpyOCH_2CH_2$ PFS), 3.30 (m, 2H; CH_2NHCOO), 3.43 (s, 3H; OCH_3), 4.40–3.51 (m, 383H; (PFS+PEO), $CH_2OC(=O)$), 4.61 (b, 2H; $tpyOCH_2$ PFS), 4.80 (b, 2H; $tpyOCH_2$ PEO), 4.93 (s, 1H; NHCOO), 7.20 (m, 4H; $H_{5,5''}$), 7.39 (m, 4H; $H_{6,6''}$), 7.81 (m, 4H; $H_{4,4''}$), 8.24 (s, 2H; $H_{3',5'}$ PFS), 8.31 (s, 2H; $H_{3',5'}$ PEO), 8.41 ppm (m, 4H; $H_{3,3''}$); UV/Vis (CH_3CN): λ (ε): 484 (17000), 304 (63000), 263 nm (90400 $mol^{-1}\,L\,cm^{-1}$); IR (ATR): $\tilde{\nu}$ = 3083, 2883 (CH tpy, CH_2 PEO backbone); 1716, 1543 (NHCOO); 1615 (C=C, C=N tpy); 1342, 1104, 840 cm^{-1} (C–O PEO backbone); GPC (RI): $M_n = 14600\,g\,mol^{-1}$, PDI = 1.07; MS (dithranol, MALDI-TOF): three distributions: $\Delta(m/z) = 242$ (PFS), $M_n = 3400\,g\,mol^{-1}$; $\Delta(m/z) = 44$ (PEO), $M_n = 3400\,g\,mol^{-1}$; diblock $m/z = 6330$.

Preparation of the aqueous micelles: PFS_{12}-[Ru]-PEO_{70} (50 mg) was dissolved in DMF (1 mL). Distilled water was added dropwise with a calibrated pipette (50 μL increments). The scattered light intensity was measured after each addition of water and plotted versus the added water volume. The cwc was determined according to the procedure previously described by Eisenberg et al.[10–12] The dropwise addition was continued until 1 mL of water had been added. The micellar solution was then placed in a dialysis bag (Spectra-Por membrane with a 6000–8000 Da cutoff). *N*,*N*-Dimethylformamide was then thoroughly eliminated by dialysis against regularly replaced distilled water. The concentration of the micelles in pure water was adjusted to 1 $g\,L^{-1}$. For some experiments, a vessel containing the micellar solution was placed in a 40 kHz (600 W) Branson ultrasonic bath for 2 h.

Light scattering: SLS experiments were carried out to determine the average molecular weight, M_w, and the radius of gyration, R_g, of the micelles. A Zimm plot analysis was used, as described in ref. [21a]. DLS data were analyzed by the cumulants method, as described elsewhere.[37] The *Z*-average diffusion coefficient over the whole set of aggregates was calculated from the first cumulant and the PDI of the aggregates was estimated from the Γ_2/Γ_1^2 ratio, where Γ_i is the *i*th cumulant. The diffusion coefficient extrapolated to zero concentration was related to the hydrodynamic diameter (D_h) by the Stokes–Einstein equation.[37] The DLS data were also analyzed by the CONTIN routine, a method which is based on a constraint inverse Laplace transformation of the data and which gives access to a size distribution histogram for the aggregates.

Acknowledgements

J.F.G. is grateful to the Action de Recherche Concertée NANOMOL 03/08-300 and to J.-F. Stasijns (UCL) for DSC measurements. B.G.G.L., A.A., and U.S.S. thank Ir. B.F.M. de Waal (SyMOChem) for a generous gift of di(*tert*-butyl)tricarbonate, Dipl.-Chem. M.A.R. Meier for MALDI-TOF MS measurements, and the Dutch Council for Scientific Research (NWO), the Dutch Polymer Institute (DPI), and the Fonds der Chemischen Industrie for financial support. I.M. and M.A.W. are grateful to Materials and Manufacturing Ontario for an EMK Grant. I.M. thanks the Canadian Government for a Canada Research Chair.

---

[1] A. Halperin, M. Tirrell, T. P. Lodge, *Adv. Polym. Sci.* **1992**, *100*, 31.
[2] G. Riess, *Prog. Polym. Sci.* **2003**, *28*, 1107.
[3] See, for example: a) L. Qi, H. Cölfen, M. Antonietti, *Nano Lett.* **2001**, *1*, 61; b) S. Klingelhöfer, W. Heitz, A. Greiner, S. Oestreich, S. Förster, M. Antonietti, *J. Am. Chem. Soc.* **1997**, *119*, 10116; c) S. Förster, M. Antonietti, *Adv. Mater.* **1998**, *10*, 195; d) J. P. Spatz, S. Sheiko, M. Möller, *Macromolecules* **1996**, *29*, 3220; e) L. M. Bronstein, S. N. Sidorov, P. M. Valetsky, J. Hartmann, H. Cölfen, M. Antonietti, *Langmuir* **1999**, *15*, 6256.
[4] S. Katayose, K. Kataoka, *Bioconjugate Chem.* **1997**, *8*, 702.
[5] A. V. Kabanov, E. V. Batrakova, V. Y. J. Alakhov, *J. Controlled Release* **2002**, *82*, 189.
[6] Y. Kakizawa, K. Kataoka, *Adv. Drug Delivery Rev.* **2002**, *54*, 203.
[7] K. Kataoka, A. Harada, Y. Nagasaki, *Adv. Drug Delivery Rev.* **2001**, *47*, 113.
[8] I. W. Hamley, *The Physics of Block Copolymers*, Oxford University Press, New York, **1998**.
[9] S. Förster, M. Antonietti, *Adv. Mater.* **1998**, *10*, 195.
[10] L. Zhang, A. Eisenberg, *Science* **1995**, *268*, 1728.
[11] a) K. Yu, A. Eisenberg, *Macromolecules* **1996**, *29*, 6359; b) K. Yu, L. Zhang, A. Eisenberg, *Langmuir* **1996**, *12*, 5980; c) K. Yu, A. Eisenberg, *Macromolecules* **1998**, *31*, 3509; d) K. Yu, C. Bartels, A. Eisenberg, *Langmuir* **1999**, *15*, 7157.
[12] L. Zhang, A. Eisenberg, *J. Am. Chem. Soc.* **1996**, *118*, 3168.
[13] See for example: B. M. Discher, Y. Y. Won, D. S. Ege, J. C. M. Lee, F. S. Bates, D. E. Discher, D. A. Hammer, *Science* **1999**, *284*, 1143.
[14] R. Djalali, S.-Y. Li, M. Schmidt, *Macromolecules* **2002**, *35*, 4282.
[15] M. Zhang, M. Drechsler, A. H. E. Müller, *Chem. Mater.* **2004**, *16*, 537.
[16] S. Minko, A. Kiriy, G. Gorodyska, M. Stamm *J. Am. Chem. Soc.* **2002**, *124*, 10193.
[17] M. Antonietti, S. Heinz, M. Schmidt, C. Rosenauer, *Macromolecules* **1994**, *27*, 3276.
[18] a) J. Tao, S. Stewart, G. Liu, M. Yang, *Macromolecules* **1997**, *30*, 2738; b) J. Ding, G. Liu, *Macromolecules* **1997**, *30*, 655.
[19] J. P. Spatz, S. Mössmer, M. Möller, *Angew. Chem.* **1996**, *108*, 1673; *Angew. Chem. Int. Ed. Engl.* **1996**, *35*, 1510.
[20] Y. Y. Won, H. T. Davis, F. S. Bates, *Science* **1999**, *283*, 960.
[21] a) J. A. Massey, K. N. Power, I. Manners, M. A. Winnik, *J. Am. Chem. Soc.* **1998**, *120*, 9533; b) J. A. Massey, K. Temple, L. Cao, Y. Rharbi, J. Raez, M. A. Winnik, I. Manners, *J. Am. Chem. Soc.* **2000**, *122*, 11577; c) J. A. Massey, M. A. Winnik, I. Manners, V. Z.-H. Chan, J. M. Ostermann, R. Enchelmaier, J. P. Spatz, M. Möller, *J. Am. Chem. Soc.* **2001**, *123*, 3147; d) L. Cao, J. A. Massey, M. A. Winnik, I. Manners, S. Riethmüller, F. Banhart, M. Möller, *Adv. Funct. Mater.* **2003**, *13*, 271.
[22] For recent reviews on the applications of PFS, see: a) I. Manners, *J. Polym. Sci. Part A Polym. Chem.* **2002**, *40*, 179; b) K. Kulbaba, I. Manners, *Macromol. Rapid Commun.* **2001**, *22*, 711.
[23] B. G. G. Lohmeijer, U. S. Schubert, *Angew. Chem.* **2002**, *114*, 3980; *Angew. Chem. Int. Ed.* **2002**, *41*, 3825.
[24] a) J.-F. Gohy, B. G. G. Lohmeijer, U. S. Schubert, *Macromolecules* **2002**, *35*, 4560; b) J.-F. Gohy, B. G. G. Lohmeijer, B. Décamps, E. Leroy, S. Boileau, J. A. van den Broek, D. Schubert, W. Haase, U. S. Schubert, *Polym. Int.* **2003**, *52*, 1611; c) V. Vogel, J.-F. Gohy, B. G. G. Lohmeijer, J. A. van den Broek, W. Haase, U. S. Schubert, D. Schubert, *J. Polym. Sci. Part A Polym. Chem.* **2003**, *41*, 3159; d) O. Regev, J.-F. Gohy, B. G. G. Lohmeijer, S. K. Varshney, D. H. H. Hubert, P. M. Frederik, U. S. Schubert, *Colloid Polym. Sci.* **2004**, *282*, 407; e) J.-F. Gohy, H. Hofmeier, A. Alexeev, U. S. Schubert, *Macromol. Chem. Phys.* **2003**, *204*, 1524.
[25] J.-F. Gohy, B. G. G. Lohmeijer, S. K. Varshney, U. S. Schubert, *Macromolecules* **2002**, *35*, 7427.
[26] J.-F. Gohy, B. G. G. Lohmeijer, U. S. Schubert, *Macromol. Rapid Commun.* **2002**, *23*, 555.
[27] J.-F. Gohy, B. G. G. Lohmeijer, U. S. Schubert, *Chem. Eur. J.* **2003**, *9*, 3472.
[28] J. Raez, R. Barjovanu, J. A. Massey, M. A. Winnik, I. Manners, *Angew. Chem.* **2000**, *112*, 4020; *Angew. Chem. Int. Ed.* **2000**, *39*, 3862.
[29] L. Cao, I. Manners, M. A. Winnik, *Macromolecules* **2001**, *34*, 3353.
[30] R. Resendes, J. A. Massey, K. Temple, L. Cao, K. N. Power-Billard, M. A. Winnik, I. Manners, *Chem. Eur. J.* **2001**, *7*, 2414.
[31] R. Resendes, J. Massey, H. Dorn, M. A. Winnik, I. Manners, *Macromolecules* **2000**, *33*, 8.
[32] X.-S. Wang, M. A. Winnik, I. Manners, *Macromol. Rapid Commun.* **2002**, *23*, 210.
[33] P. Zhang, J. S. Moore, *J. Polym. Sci. Part A Polym. Chem.* **2000**, *38*, 207.
[34] H. W. I. Peerlings, E. W. Meijer, *Tetrahedron Lett.* **1999**, *40*, 1021.
[35] a) M. A. R. Meier, B. G. G. Lohmeijer, U. S. Schubert, *Macromol. Rapid Commun.* **2003**, *24*, 852; b) M. A. R. Meier, B. G. G. Lohmeijer, U. S. Schubert, *J. Mass Spectrom.* **2003**, *38*, 510.
[36] L. Zhang, H. Shen, A. Eisenberg, *Macromolecules* **1997**, *30*, 1001.
[37] B. J. Berne, R. J. Pecora, *Dynamic Light Scattering*, Wiley, Toronto, **1976**.
[38] M. Schmidt, W. H. Stockmayer, *Macromolecules* **1984**, *17*, 509.
[39] M. Al-Hussein, B. G. G. Lohmeijer, U. S. Schubert, W. H. de Jeu, *Macromolecules* **2003**, *36*, 9281.
[40] U. S. Schubert, C. Eschbaumer, O. Hien, P. R. Andres, *Tetrahedron Lett.* **2001**, *42*, 4705.

Received: March 8, 2004